Contents lists available at ScienceDirect

Physics in Medicine

journal homepage: www.elsevier.com/locate/phmed

Flexible perovskite based X-ray detectors for dose monitoring in medical imaging applications

Hardeep Singh Gill[a,b], Bassem Elshahat[b,c], Akshay Kokil[a], Lian Li[d], Ravi Mosurkal[d], Piotr Zygmanski[e], Erno Sajo[b], Jayant Kumar[a,b,*]

[a] Center for Advanced Materials, University of Massachusetts Lowell, Lowell, MA 01854, USA
[b] Department of Physics and Applied Physics, University of Massachusetts Lowell, Lowell, MA 01854, USA
[c] Department of Medical Imaging, Royal Jubille Hospital, Vancouver Island Authority, Victoria, BC V8R 1J8, Canada
[d] Bio-science Team, US Army Natick Soldier Research, Development & Engineering Center, Natick, MA 01760, USA
[e] Department of Radiation Oncology, Brigham and Women's Hospital & Dana Faber Cancer Institute, Harvard Medical School, Boston, MA 02115, USA

ARTICLE INFO

ABSTRACT

Organometallic halide perovskite materials are attracting considerable interest for high performance photovoltaic and photodetector applications due to their exceptional opto-electronic properties and easy processing capability. The high atomic numbers (Z) of their constituents also make these materials suitable for X-ray detection. Here we report on the direct detection of X-ray induced photocurrents in flexible organolead halide perovskite based detectors. The electrical response of the detectors was found to be linear with the radiation dosage. These perovskite based radiation detectors were about 550% more sensitive than commonly used amorphous silicon solar devices. The high sensitivity to the X-rays could be attributed to the high Z constituents and large charge carrier mobility. Our results indicate that the perovskite materials are promising candidates for direct X-ray detectors.

1. Introduction

Sensitive detection of X-rays offers broad applications in many diverse fields, such as medical diagnostic imaging, industrial non-destructive testing and homeland security. In many applications X-ray detectors with large active areas are needed with sufficient sensitivity. The current X-rays detection technologies used in flat-panel detectors are based on non-flexible and expensive silicon based detectors, charge coupled devices (CCD) or CMOS devices coupled with a scintillation layer [1–4]. Presence of the scintillation layer introduces multiple imaging challenges related to lower response times and diminished signal to noise ratios at high X-ray intensities [5]. In addition, the fabrication of large area flexible silicon based devices is a challenge. Hence, the development of flexible direct (i.e. scintillator free), real-time conformal X-ray detectors are highly desirable. In particular, development of thin-film flexible X-ray detectors, which conform to the shape of the object would also provide the detection of important spatial X-ray gradient used in image guided radiation therapy (IGRT) and intensity modulated radiation therapy (IMRT). In the last two decades, owing to their flexibility and ease of fabrication, organic semiconductors have received attention for thin film photovoltaics

(PVs), optical sensing and recently been proposed for X-ray detection. The devices based on flexible organic semiconductors offer many advantages, e.g., tissue equivalence and high extinction coefficients in the visible region [6–14]. However, the organic materials that were used for this purpose have low average atomic numbers (Z), making them transparent to X-rays thus severely limiting their applications in X-ray detection. To increase the signal in organic semiconductor-based X-ray detectors, there is a need to raise the attenuation of X-rays in the polymer film. Hybrid organometallic halide perovskite compounds have rapidly emerged to the forefront of PV research exhibiting high power-conversion efficiencies and the promise of low-cost fabrication in devices [15]. More importantly, high charge carrier mobilities, long charge carrier lifetime and high exciton diffusion length have been observed in perovskite films [16,17]. This strongly suggests a potential of this class of materials for photodetector applications [18,19]. Recently, Huang et al. reported gammavoltaic effect in single crystal $CH_3NH_3PbI_3$ with an intense Cs-137 source [20]. This indicates that the high-Z of the constituents (which result in an increased X-ray absorption cross-section) can also render efficient absorption of X-rays in films. Therefore, as reported by Haotong and et al. a detector made of a very thin (few hundred nanometers) layer of perovskite material is
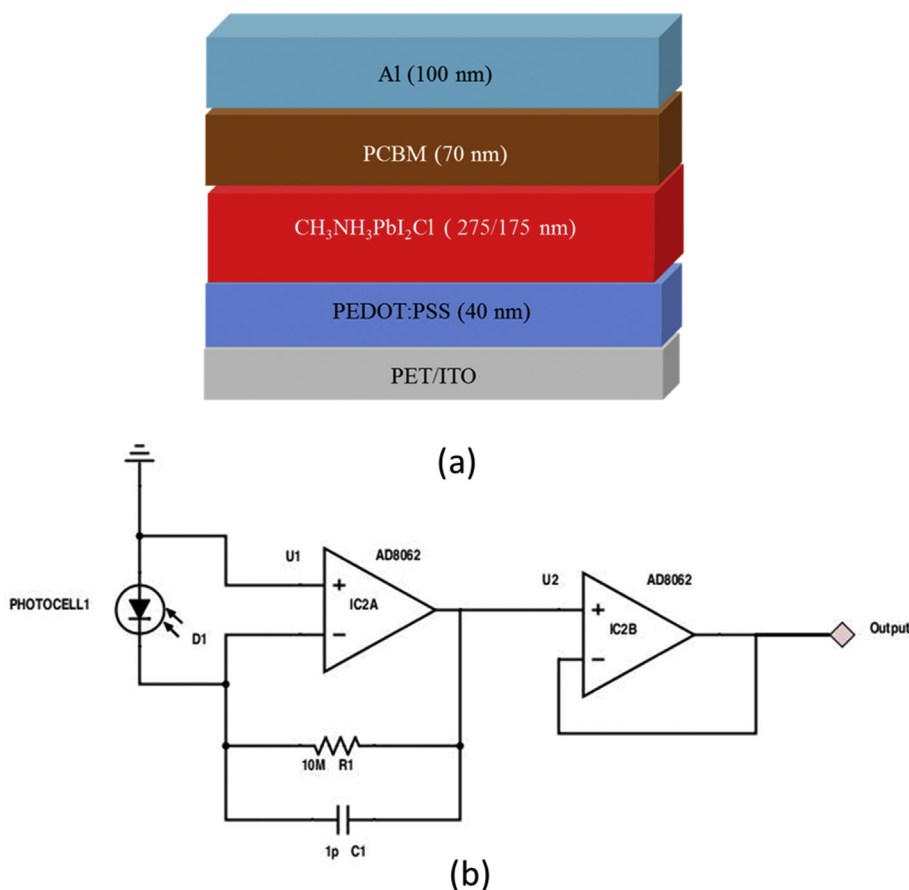

Fig. 1. (a) Schematic diagram of the perovskite based X-ray detector. X-rays were normally incident on the device through ITO/PET substrate. *Dimensions are drawn not to scale. (b) A circuit diagram of the device adapted from reference 23.
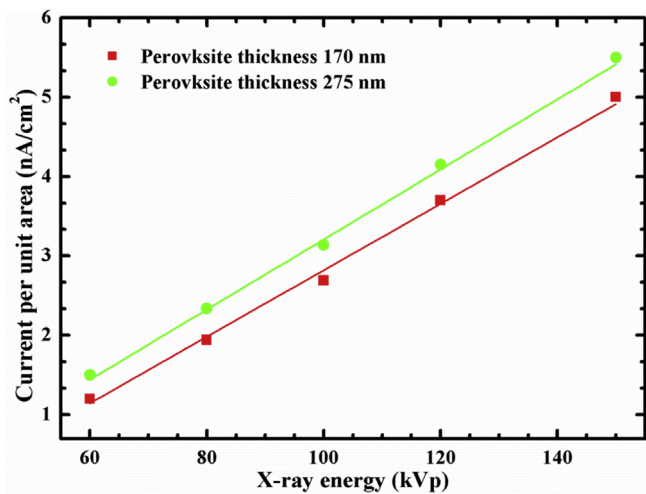

Fig. 2. X-ray generated current density as a function of beam energy for two perovskite based devices of different thicknesses. Solid lines are least square fits. The error range on the data points is ± 0.05 nA, which is approximated by the size of the symbols.

Fig. 3. Reproducibility and response of a perovskite device with thickness 270 nm for four successive but different exposure times: 1, 1.6, 2.5 and 3.0 s. Sampling time was 0.9 ms.

sufficient to generate a measurable signal when exposed to X-rays [21]. In this work, we report the direct detection of X-ray induced photo-currents in organo-lead halide perovskite based devices. We have shown that flexible X-ray detectors fabricated using this material are about 550% more sensitive than commonly used amorphous (a-Si) based solar cells. These results clearly indicate that the organo-lead halide perovskite based detectors are promising candidates for low-cost
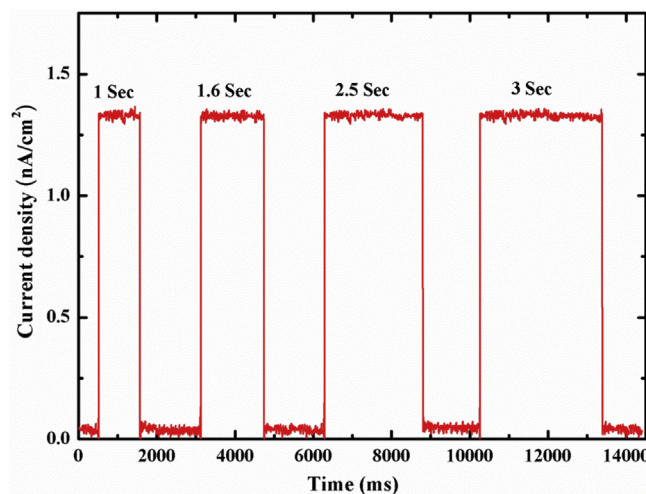
thin-film flat panel or curved surface detector arrays.

2. Experimental details

A set of low temperature solution processed flexible organolead halide perovskite based detectors with two different thicknesses were fabricated to evaluate their response to X-rays. The planar device structure of the detector and a circuit diagram of the device are shown
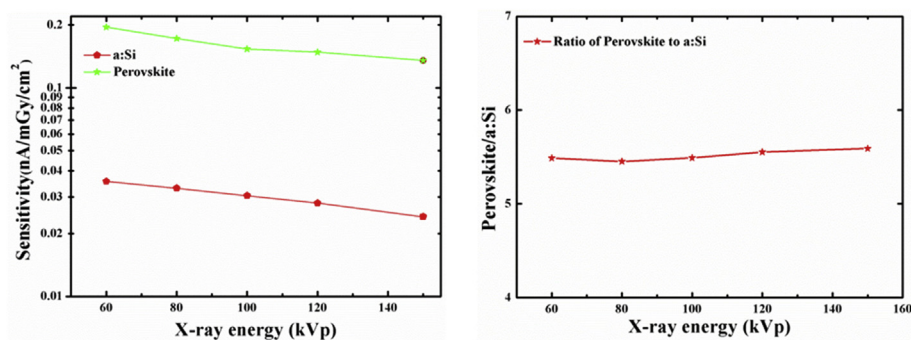
Fig. 4. Comparison of the sensitivity of the fabricated perovskite (270 nm) based detector and a commercial a:Si solar cell. A (left): Measured device current as a function of beam energy and normalized to detector size and beam output. B (right): Ratio of net current shown in (A). Data for a:Si were adapted without alteration from reference 23. Propagated relative experimental uncertainties at the ± 1 σ level are between 0.1% and 3.4%, and are within the line thicknesses.

in Fig. 1. Poly (3,4-ethylenedioxythiophene):poly(4-styrenesulfonate) (PEDOT:PSS) (hole transporting material, p-type layer) were first spin-coated at 2500 rpm on indium tin oxide (ITO) coated poly (ethylene-terephthalate) (PET) substrates (sheet resistance of 50 Ω/), and dried at 75 °C for 2 h. $CH_3NH_3PbI_2Cl$ film was then deposited by spin-casting at 2500 rpm (170 nm), 1500 rpm (275 nm); and was subsequently heated at 70 °C for 30 min. $CH_3NH_3PbI_2Cl$ was then sandwiched between the PEDOT:PSS film and [6,6]- phenyl C_{61}-butyric acid methyl ester (PCBM) (electron-transporting material, n-type layer) by spin casting the PCBM (70 nm) film on top of $CH_3NH_3PbI_2Cl$ film. An aluminum (Al) film (100 nm) was finally deposited through a shadow mask (0.5 cm^2) to complete the device fabrication. The fabricated devices were encapsulated using epoxy to avoid any immediate degradation. Devices based on similar configuration have been demonstrated with good photovoltaic performance in previous reports [21].

Raw signal from organolead halide perovskite based X-ray detectors was sampled using two types of data acquisition devices (DAQ): a USB wireless transceiver system (eZ430-RF2500 Texas Instruments) and a 128-channel current to digital converter ADAS1128 by Analog Devices [22]. The radiation source was a Varian Ximatron™ KVp X-ray system with a tungsten-rhenium target and the source to sample distance was 100 cm. For comparison to a commercially available radiation detector, which is used as industry standard in medical physics measurements, an IBA MagicMaX™ meter was used separately to measure the air kerma. The experimental setup for the X-ray generation and sample exposure used in our readout system has been described elsewhere.[23] All the samples through PET/ITO side were exposed to X-ray energies ranging from 60 to 150 kVp at 200 mA current for 1 s. This exposure time was selected, so that signal stability of the photocells could be tested.

3. Results and discussion

Absorption of X-rays in the active layer of the device leads to the creation of electron-hole pairs. Normally, in solid-state devices the generated electrons and holes are collected at their respective electrodes by the application of an external electric field. However, in our thin-film detectors an inherent field is formed resulting from the difference in the work functions of the electrodes, thus no external electric field is required for charge collection. This can significantly simplify the data acquisition electronics in this detection technique [24]. Fig. 2 shows the net photocurrent per unit area as a function of X-ray energy of the tested configurations. The X-ray induced photocurrent from the fabricated samples increases as the dose rate of incident X-rays increases. As depicted in Fig. 2, the fabricated devices exhibited the linear dependence of induced currents on the X-ray energy. The measured photocurrent ranged from approximately 1.1 to 5.6 nA/cm^2 for 60 to 150 kVp, corresponding to about 0.22–0.15 nA per mGy air kerma, respectively. From our results, it is obvious that X-ray response greatly depends on the active layer thickness. The devices with thick active layer produced good response. The observed enhancement in sensitivity of detectors with increased thickness is due to better absorption of X-ray

in the thicker layer generating more electron-hole pairs from the active layer. Therefore, optimum selection of active layer thickness is crucial for the fabrication of X-ray detector.

The time-dependent X-ray response for the device with perovskite layer thickness 270 nm is investigated to determine the stability and reproducibility of the signal after repeated exposures. X-ray tube was adjusted to provide 200 mA current at 60 kVp energy. The fabricated sample was irradiated for four different exposure times, 1.0, 1.6, 2.6, and 3.0 s with 1 s resting period between each exposure. The sampling time was 0.9 ms. Fig. 3 shows the fabricated detector response as a function of time during the repeated exposures. The induced photocurrent has a good stability over the period of exposure, and it remained nearly constant at 1.34 ± 0.02 nA/cm^2. The integrated signal was also linear with the exposure time. Signal rise time varied between 5 and 6 ms with an average of 5.6 ± 0.4 ms. When the X-rays are switched off, the induced photocurrent drops sharply with an average characteristic time constant of 5 ± 0.3 ms after irradiation. Upon prolonged exposure times, there is no observable loss of X-ray sensitivity, indicating that the fabricated organo-lead halide perovskite based detector shows no sign of radiation damage. These results demonstrate that the fabricated devices can be repeatedly operated for prolonged exposure times under extreme conditions of radiations as no sign of radiation damage is observed.

To compare the performance with a commercially available a-Si based solar cell (SP-13; PowerFilm Inc., Ames, IA) was used. The organo-lead halide perovskite based device and the a-Si solar cell were exposed to the same X-ray energies for the same duration. As shown in Fig. 4 the signal obtained by a fabricated organo-lead halide perovskite based device has a similar dependence on the X-ray tube energy as the a-Si thin film solar cell [23]. The overall performance of the organo-lead halide perovskite based detector is significantly better than a same sized commercial a-Si solar cell. Fig. 4b shows the ratio of organo-lead halide perovskite based PV signal to that of the commercial a-Si based solar cell, adjusted for beam output as function of X-ray energy. The ratio is nearly constant at 5.50 ± 0.05 across all tested beam energies. Further improvements in sensitivity could be achieved by optimizing the thickness of metal film and using the plastic substrates of lower sheet resistance.

4. Conclusions

In summary, we have reported the fabrication of organo-lead halide perovskite based detectors for real time X-ray detection. It has been shown that the organo-lead halide perovskite based detectors have sensitivity of 550% higher than commercially available a-Si solar cell. The possibility of detecting X-rays with energies relevant to medical imaging applications opens up the potential for these detectors to be used in detection and dosimetry applications in diagnostic imaging.

Acknowledgements

References

[1] S. Kasap, J.B. Frey, G. Belev, O. Tousignant, H. Mani, J. Greenspan, L. Laperriere, Sensors 11 (2011) 5112.

[2] K.M. Oh, J.W. Shin, S.U. Heo, J.S. Kim, J.G. Park, S.H. Nam, J. Instrum. 9 (2014) P01010.

[3] J.P. Moy, Nucl. Instrum. Meth. Phys. Res. 442 (2000) 26.

[4] W. Zhao, I. Blevis, S. Germann, J.A. Rowlands, D. Waechter, Z. Huang, Med. Phys. 24 (1997) 1834.

[5] C.W.E. van Eijk, Phys. Med. Biol. 47 (2002) R85.

[6] D. Natali, M. Sampietro, Nucl. Instrum. Meth. Phys. Res. A 512 (2003) 419.

[7] T. Agostinelli, M. Campoy-Quiles, J.C. Blakesley, R. Speller, D.D.C. Bradley, J. Nelson, Appl. Phys. Lett. 93 (2008) 203305.

[8] P.E. Keivanidis, N.C. Greenham, H. Sirringhaus, R.H. Friend, J.C. Blakesley, R. Speller, M. Campoy-Quiles, T. Agostinelli, D.D.C. Bradley, J. Nelson, Appl. Phys. Lett. 92 (2008) 023304.

[9] J.W. Kingsley, A.J. Pearson, L. Harris, S.J. Weston, D.G. Lidzey, Org. Electron. 10 (2009) 1170.

[10] F.A. Boroumand, M. Zhu, A.B. Dalton, J.L. Keddie, P.J. Sellin, J.J. Gutierrez, Appl. Phys. Lett. 91 (2007) 033509.

[11] S. Satapathi, H.S. Gill, L. Li, L. Samuelson, J. Kumar, R. Mosurkal, Appl. Surf. Sci. 323 (2014) 13.

[12] C.A. Mills, H. Al-Otaibi, A. Intaniwet, M. Shkunov, J.L. Keddie, P.J. Sellin, J. Phys. D 46 (2013) 275102.

[13] A. Intaniwet, C.A. Mills, P.J. Sellin, M. Shkunov, J.L. Keddie, ACS Appl. Mater. Interfaces 2 (2010) 1692.

[14] F. Arca, S.F. Tedde, M. Sramek, J. Rauh, P. Lugli, O. Hayden, Sci. Rep. 3 (2013) 1324.

[15] L.M. Liu, M.B. Johnston, H.J. Snaith, Nature 501 (2013) 395.

[16] S.D. Stranks, G.E. Eperon, G. Grancini, C. Menelaou, M.J. Alcocer, T. Leijtens, L.M. Herz, A. Petrozza, H.J. Snaith, Science 342 (2013) 341.

[17] C. Wehrenfennig, G.E. Eperon, M.B. Johnston, H.J. Snaith, L.M. Hertz, Adv. Mat. 26 (2014) 1584.

[18] Y.M. Dou, J. Yang, Z. You, W.H. Hong, G. Chang, Li, Y. Yang, Nat. Commun. 5 (2014).

[19] M. Spina, M. Lehmann, B. Nafradi, L. Bonvin, R. Gaal, A. Magrez, E. Horvath, Small 11 (2015) 37.

[20] Q. Dong, Y. Fang, Y. Shao, P. Mulligan, J. Qiu, L. Cao, J. Huang, Science 347 (6225) (2015) 967–970.

[21] H. Wei, Y. Fang, P. Mulligan, W. Churiazzi, H.H. Fang, C. Wang, B.R. Ecker, et al., Nat. Photon. 10 (2016).

[22] H.S. Gill, A. Kokil, L. Li, R. Mosurkal, J. Kumar, Proc. SPIE 9184 (2014) 918418.

[23] P. Zygmanski, C. Abkai, Z. Han, Y. Shulevich, D. Menichelli, J. Appl. Clin. Med. Phys. 15 (2014) 2.

[24] B. Elshahat, H.S. Gill, I. Filipyev, S. Shrestha, J. Hesser, J. Kumar, A. Karrellas, P. Zygmanski, E. Sajo, Med. Phys. 42 (2015) 7.